Ruisheng Guo and Prof. Feng Zhou
Superhydrophobic Surfaces for Drag Reduction

SpringerReference

Superhydrophobic Surfaces for Drag Reduction

## Synonyms

Low friction surfaces

Definition

Superhydrophobic surfaces for drag reduction utilize a surface with superhydrophobic properties to reduce friction of a liquid flowing on it. Superhydrophobic surfaces are normally composite surfaces consisting of a large fraction of trapped air, thus generating boundary slippage and bringing about a shear-free air-water interface. Drag reduction significantly contributes energy saving and device efficiency in liquid transportation or other tribological systems.
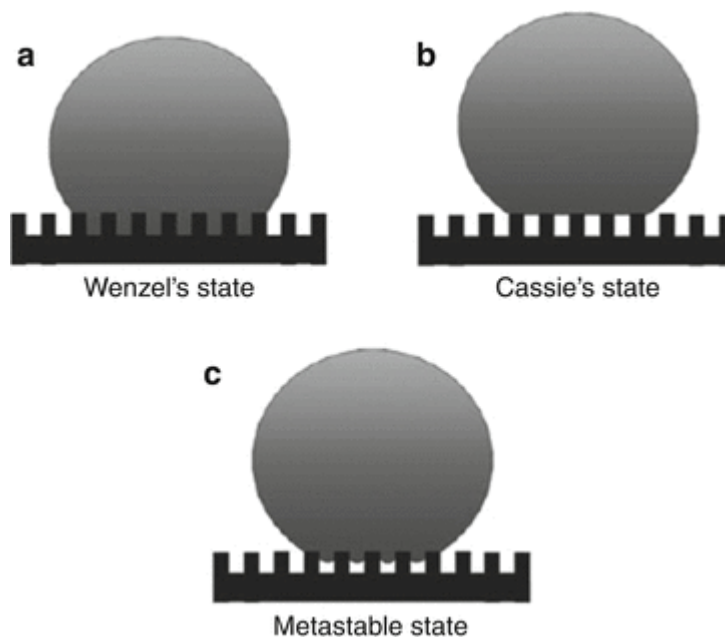
Scientific Fundamentals

Basic Theory of Superhydrophobicity

Wettability is defined as the tendency of one fluid to spread on or adhere to a solid surface in the presence of other immiscible fluids. The common situation is that water displaces air on the solid surface. Wettability is characterized by the contact angle between the solid and a drop of liquid as shown in Fig. 1a. If the liquid wets the surface (referred to as the hydrophilic/oleophilic surface), the value of the contact angle is $0° < θ < 90°$, whereas, if the liquid does not wet the surface (referred to as a hydrophobic/oleophobic surface), the value of the contact angle should be $90° < θ < 180°$. The term hydrophobic/philic is usually used to describe the contact of a solid surface with water, while the term "oleophobic/philic" refers to wetting by oil and organic liquids. A surface is considered superhydrophobic/superoleophobic if $θ$ is greater than 150° and contact angle hysteresis is low. Contact angle hysteresis defines the difference between advancing and receding contact angles when a drop of liquid starts to move on a tilting surface as shown in Fig. 1b, and it reflects the adhesion behavior between liquid and solid (higher contact angle has stronger adhesion).
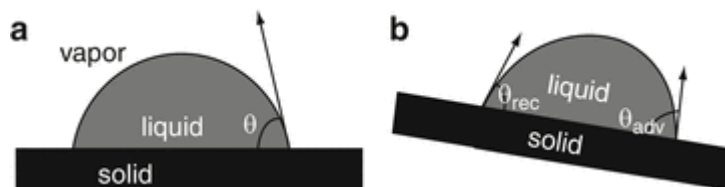
Superhydrophobic Surfaces for Drag Reduction, Fig. 1 (a) Contact angle between the solid and liquid surfaces, (b) contact angle hysteresis ($θ_{adv}$ - $θ_{rec}$)

In fact, microscopically, there are different contact modes at the interface of liquid and solid. Figure 2a shows the Wenzel's state, where the droplet has intimate contact with the surface features. The adhesion on liquid/solid interface is obviously large. Figure 2b displays Cassie's state, where the droplet suspends on the top of the rough features with air trapped underneath; thus, the droplet is unstable and can roll off easily. However, in most cases, a water droplet may partially wet a surface and assume an intermediate state between Wenzel and Cassie states. Such an intermediate state of solid/liquid contact is referred as a metastable state (see Fig. 2c). This indicates that the external physical conditions can strongly affect the transition between the Cassie and Wenzel state, including the height of nanopillars, the spacing between pillars, and the intrinsic contact angle. Furthermore, transition between the two states could be achieved on the same microstructured surface when external stimuli (like a pressing force) exist.

Ruisheng Guo and Prof. Feng Zhou
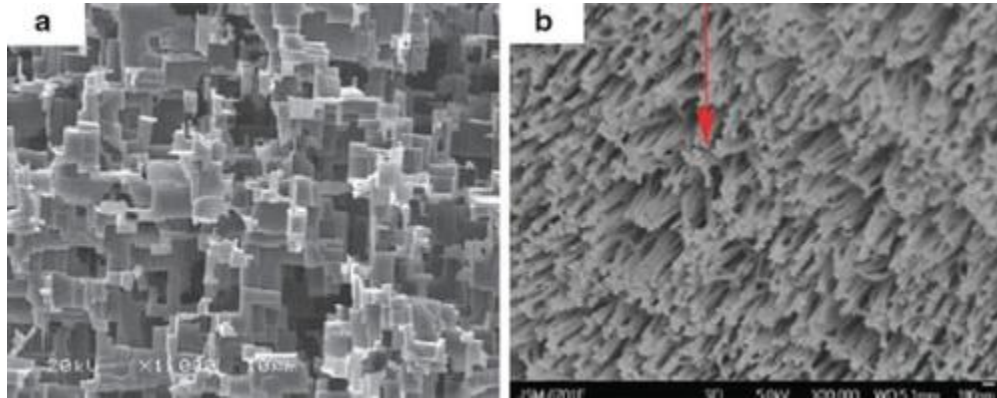Superhydrophobic Surfaces for Drag Reduction

SpringerReference

Superhydrophobic Surfaces for Drag Reduction, Fig. 2 Contact state of interface between liquid and solid (a) Wenzel's state, (b) Cassie's state, (c) Metastable state (Liu and Jiang 2010)

Fabrication of Superhydrophobic Surfaces

Superhydrophobicity has attracted a great deal of attention both in fundamental research and for potential applications including self-cleaning windows, windshields, exterior paints for buildings and navigation of ships, utensils, and antifouling. The focus here is on using a superhydrophobic surface for drag reduction.

Surface roughness plays a critical role in surface wettability. It influences the behaviors of liquid droplets both thermodynamically and hydrodynamically. Enhanced surface roughness will increase the surface's static contact angle and make the surface water repellent. However, it will sometimes increase the contact angle hysteresis and make it difficult for the droplet to roll off. Hence, it is very important to design and optimize surface roughness to obtain superhydrophobic surfaces with high contact angle and low contact angle hysteresis. To obtain the enhanced Cassie state superhydrophobicity, the study and simulation of biological objects with desired properties is referred to as "biomimetics." Biomimetics involves looking for engineering solutions from nature, mimicking them, and implementing them in practice. The lotus leaf is a typical example. The lotus emerges totally clean from muddy water. By observing the surface morphology, people found that the cooperation of the surface micro- and nanometer hierarchical structures and low-surface-energy hydrophobic wax-like material contributes to the superhydrophobicity. This finding is considered a great step forward in the field for the fabrication of artificial superhydrophobic surfaces. On the basis of our understanding of nature, a number of artificial hydrophobic surfaces have been fabricated with low surface energy materials and hierarchical structures using electrochemical methods, colloidal particles, photolithography, soft lithography, plasma treatment, self-assembly, and imprinting. As such an example, Wu et al. (2009) prepared a super-repellent surface by forming multiple-facet supported alumina nanowires with hierarchical micro/nanostructures (Fig. 3), which showed super-repellency towards a broad range of liquids after post-modification with perfluorosilane, including water, hexadecane, silicone oil, and crude oil. This provides a good example of biomimicing beyond nature since the superoleophobic surfaces are rarely found in nature. The complicated surface structure can be replicated into conventional polymeric coatings and materials (Liu et al. 2009), exhibiting superhydrophobicity and superolephobicity as well after additional surface treatment. Inspired by nature, people have created a number of functional superhyophobic materials. For example, anisotropic superhydrophobic surfaces are inspired by pigeon and goose feathers or bamboo leaves, superhydrophobic antifogging coatings are inspired by mosquito eyes; antireflective surfaces by moth eyes and cicada wings; and superhydrophobic surfaces that are highly adhesive mimick rose petals and gecko feet (Liu et al. 2010).

Ruisheng Guo and Prof. Feng Zhou
Superhydrophobic Surfaces for Drag Reduction

SpringerReference

Superhydrophobic Surfaces for Drag Reduction, Fig. 3 Micro- and nanoscale hierarchical alumina (a) microscale multi-facet aluminum, (b) nanowire forests on a multi-facet mattress

Fundamental of Flow

There are mainly two types of flow: laminar and turbulent. In a cylindrical conduit one can visualize the laminar flow as a series of co-axial cylinders oriented along the flow direction; such a flow structure is known as telescopic shear. The central part of the fluid has the highest velocity U. The velocity on the wall is zero, with the intermediate velocities in-between. A schematic representation is shown in Fig. 4a. Another way to create laminar flow is using two parallel plates with one moving and one stationary, as shown in Fig. 4b.
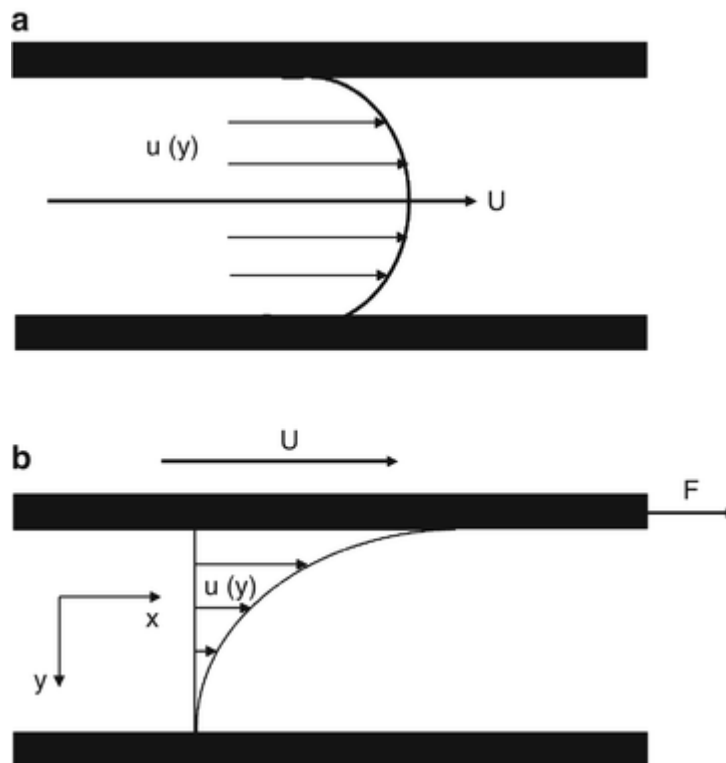
Superhydrophobic Surfaces for Drag Reduction, Fig. 4 (a) Laminar flow at velocity u in a cylindrical conduit, (b) laminar flow between parallel plates. The shearing force F acts on the top plate as indicated. The velocity u decreases going down along the vector y since the velocity at the bottom plate is necessarily 0 (Modified from (Brostow 2008))

For the second mode, the fluid has the motion imposed by an applied shearing force F. When the up plate moves at the velocity U seen in Fig. 4b, velocities of fluid go down vertically along the y-axis from U (adjacent to the moving plate) to 0 (adjacent to the stationary plate). The following equation can be applied:

Ruisheng Guo and Prof. Feng Zhou
Superhydrophobic Surfaces for Drag Reduction

SpringerReference

$$F = \mu \frac{U}{h} A,$$ (1)

where μ is the viscosity of fluid, A is the surface area to which the force is applied, h is the distance between parallel plates, and U/h is the vertical velocity gradient. The shear stress т can be expressed,

$$\tau = \frac{F}{A} = \mu \frac{U}{h},$$ (2)

Generically, when velocity distribution of u(y) is at y site far from the stationary wall, the shear stress is

$$\tau = \frac{\mu \, du}{dy},$$ (3)

where du/dy is velocity gradient.

Reynolds number (Re) is normally used to discriminate between laminar flow and turbulent flow. For cylindrical conduit flow,

$$Re = \frac{D u_{av} \rho}{\mu},$$ (4)

where D is the cylindrical conduit diameter, u_{av} is the average flow velocity, and ρ is the fluid mass density. For flow over a flat plate,
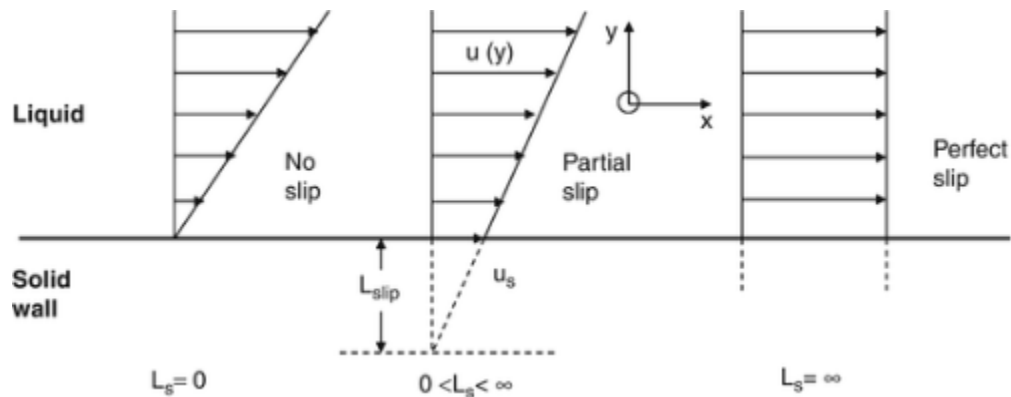
$$Re = \frac{L u_{av} \rho}{\mu},$$ (5)

where L is the length of flat plate. In general, natural transition occurs from laminar flow to turbulent flow regimes near a Reynolds number around 4,000 for cylindrical conduit flow and 500,000 for flow over a flat plate (Dean and Bhushan 2010). For values of Re much less than the above transition values (i.e., critical Reynolds number), flow is laminar. For larger Re values, the flow is turbulent.

Superhydrophobic Surfaces for Drag Reduction

The traditional view believes that no-slip boundary condition at the fluid/solid interface is an idealized paradigm, which assumes moderately strong attractive forces between the fluid and the wall. Thereby, the fluid atoms in bulk in attaining momentum and energy states differ from those of the solid boundary atoms in proximal contact. However, effects of surface tension, liquid evaporation, porosity, osmotic transport, van der Waals forces, and electrostatic forces may potentially result in true or apparent deviations from this classical picture. Even from a pure mathematical viewpoint, slip at the interface appears to be a more acceptable general notion than that of no-slip, since no-slip is a special case of slip with the magnitude of slip equal to zero! This fact was recognized by Navier more than a century ago, when he first introduced the general notion of boundary slip by defining a slip length (L_S) as the distance behind the interface at which the fluid velocity extrapolates to zero (see Fig. 4). And the slip velocity, u_S, is proportional to the shear rate experienced by the fluid at the wall

$$u_S = L_S \frac{\partial u}{\partial y}.$$ (6)

In fact, the situations of $L_S = 0$ and $L_S = \infty$ are ideal cases, slip length is between 0 and ∞ in most situation (Fig. 5) (Chakraborty 2010).

Ruisheng Guo and Prof. Feng Zhou
Superhydrophobic Surfaces for Drag Reduction

SpringerReference

Superhydrophobic Surfaces for Drag Reduction, Fig. 5 Concept of slip parameterized by the slip length, L_S (Modified from (Chakraborty 2010))

The slip effect on the surface entails meaningful drag reduction for various flow conditions. Considering the situation of two parallel plates as shown in Fig. 4b, if one of the two surfaces has a slip length L_S, the drag reduction can be estimated as

$$\frac{\tau_{slip}}{\tau_{no-slip}} = \frac{1}{1+(L_S/h)},$$ (7)

where τ_{slip} and $\tau_{no-slip}$ are the shear stresses at a wall when slip and no-slip boundary conditions are applied, respectively. In addition, according (7) the drag reduction can be calculated

$$D_R = \frac{\tau_{no-slip} - \tau_{slip}}{\tau_{no-slip}}.$$ (8)

Large drag reduction can be obtained as the gap between the plates becomes smaller, especially down to the range comparable to the slip length.

Usually, the rough structure of superhydrophobic surface is at the microscale. Due to the formation of space between solid posts, moderate roughness can lead to Cassie state contact between liquid and solid. It prevents the water from moving into the space, resulting in an air-water interface that is essentially close to shear-free. The resulting surface possesses a composite interface where momentum transfer with the wall occurs only at liquid-solid and not at liquid-vapor interfaces. Therefore, effective slippage will appear at the interface of liquid and solid. Simultaneously, experiments demonstrated that a vanishing slip length is found in the Wenzel state when the liquid impregnates the surface (Joseph et al. 2006). Therefore, superhydrophobic coatings with moderate patterning can result in an appreciable decrease of drag when liquid flows on the solid surface. Many experimental and numerical studies have reported that hydrophobic surfaces allow a noticeable slip ranging from nanometers to a micron in slip length and achieve drag reduction.

Application Study

Wetting-Related Drag Reduction

Choi et al. (Choi and Kim 2006) reported in detail about the design of superhydrophobic surface structures. They imagine Couette flow (fluid flows over a flat plate) in which an air layer separates liquid from a wall by the sharp tips of the hydrophobic posts, as shown in Fig. 6. Riding mainly over air, the liquid is expected to flow over the solid surface experiencing little friction. If one neglects the post structures (as an ideal case), a slip length L_S due to the pure air layer of thickness b, which is seen as the thickness of boundary layer, can be represented by

Ruisheng Guo and Prof. Feng Zhou
Superhydrophobic Surfaces for Drag Reduction

SpringerReference

$$L_S = b(\mu_l/\mu_a - 1),$$ (9)

where μ_l and μ_a are the viscosities of liquid and air, respectively (Vinogradova 1995). A large effective slip is expected due to the sizable viscosity difference between liquid and air, larger with a thicker air layer. For example, if the liquid is water and the air layer is 1 μm thick, the slip length would be 54 μm, disregarding the deviation from continuum at this scale.
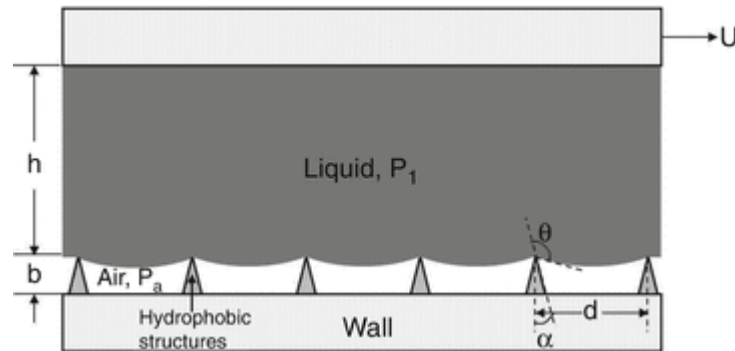
Superhydrophobic Surfaces for Drag Reduction, Fig. 6 Concept of large effective slip by a nanoengineered superhydrophobic surface in Couette flow. Liquid sits on hydrophobic structures by surface tension. The majority of the liquid boundary is with air, where shear stress is much smaller (Modified from (Choi and Kim 2006))

For the design of the surface structures, consider conical posts of height b and cone angle α as shown in Fig. 6. The posts are assumed to form a square array with a pitch d. The meniscus is assumed to be of a spherical shape with contact angle θ (or advancing contact angle θ_A when the liquid pressure increases) on the side surfaces of the posts, balancing with the liquid pressure. The posts need to be tall enough so that the meniscus does not touch the bottom surface between posts. The posts also need to be populated densely enough, i.e., the pitch should be small enough so that the surface tension of the warped meniscus withstands the pressure in the liquid. If the pitch is low or loose, with increasing pressure, the state between liquid and solid will change from the Cassie state to the Wenzel state with liquid entering the space between pitches. So slip velocity reduces rapidly and loses the effect of drag reduction. By a simple geometrical calculation and the Laplace-Young equation, the post height b and the interpost pitch d to hold up the liquid meniscus against the pressure of liquid over air ($\Delta P = P_l - P_a$) can be obtained as

$$b > \frac{1 - \sin(\theta_A - \alpha)}{\sqrt{2}|\cos(\theta_A - \alpha)|}d, \quad d < 2\sqrt{2}\sigma\frac{|\cos(\theta_A - \alpha)|}{\Delta P},$$ (10)

where σ is the surface tension of the liquid-air interface. For example, if the liquid is water (σ = 0.0727 N/m at 20°C), ΔP is 0.1 MPa (~1 atm), and (θ_A - α) is 120°, the pitch d should be less than 1 μm, and the post height b should be larger than ~0.2 μm. It is further desired to make the posts sharp at the tip so that the liquid/solid contact area is minimized and slender in shape so that the contribution of air is maximized. Equation (10) serves as a key guideline in the design of proper geometry for the purpose at hand. According to this equation, the hydrophobic nanoturf surface was fabricated with 1-2 μm height and 0.5-1 μm pitch on a silicon wafer that was modified with Teflon by spin coating. Measured through a cone-and-plate rheometer system, the surface has demonstrated slip effects: a slip length of 20 μm for water and 50 μm for 30 wt.% glycerin liquid.

The above-discussed drag reduction is only limited to laminar flow. In turbulent flow, drag reduction has also been observed in experiments. Fundamentally, the effective reduction in solid-liquid boundary as a superhydrophobic drag reduction mechanism should be independent of whether the flow is laminar or turbulent. In turbulent flows, a thin viscous-dominated sublayer exists very close to the wall. It extends to a height, measured in terms of wall units, viscous lengths, of

Ruisheng Guo and Prof. Feng Zhou
Superhydrophobic Surfaces for Drag Reduction

SpringerReference

$$y^+ = y/u\sqrt{\tau_w/\rho} = 5. \tag{11}$$

where y is the height above the wall, v is the kinematic viscosity, τ_w is the wall shear stress, and ρ is the fluid density. In the viscous sublayer, the mean velocity increases linearly with position, $u^+ = y^+$. Changes in momentum transfer to the viscous sublayer can have a dramatic influence on the entire turbulent flow and can result in drag reduction for superhydrophobic surfaces.

Daniello et al. (2009) fabricated two types of superhydrophobic microridge geometries, which have been tested over a range of mean Reynolds numbers 2,000 < Re < 9,500. Two geometries with 50% shear-free air-water interface coverage were considered. The first contains microridges d = 30 μm wide and spaced w = 30 μm apart (30-30) and the second contained microridges d = 60 μm wide and spaced w = 60 μm apart (60-60). Particle image velocimetry and pressure drop measurements were used to observe significant slip velocities, shear stress, and pressure drop reductions corresponding to drag reductions approaching 50%. At a certain Reynolds number, drag reduction increases with increasing feature size and spacing. And drag reduction promotes with further increasing Reynolds number.

Then they made further analysis for above results. Although the viscous sublayer thickness remains fixed in wall units, in dimensional form the thickness of the viscous sublayer decreases with increasing Reynolds number as

$$y_{vsl} = 5u\sqrt{\rho/\tau_w}$$. Close to the wall, where viscous stresses dominate, the influence of the shear-free air-water interface extends to a distance roughly equal to the microridge spacing, w, into the flow. Thus, for the superhydrophobic surface to impact the turbulent flow, the microridge spacing must approach the thickness of the viscous sublayer, y_{vsl}, or in other words $w^+ = y^+ \approx 5$. As seen in Fig. 7, the microfeature spacing in wall units is at least $w^+ > 0.75$ for all the 30-30 surfaces and $w^+ > 2.4$ for the 60-60 surfaces. This means that the microfeature spacing is minimally 15-50% of viscous sublayer thickness almost immediately after the turbulent transition (critical Reynolds number is about 2,500). Hence for 30-30 and 60-60 ridges, drag reduction is noticed almost as soon as a turbulent flow develops. As the Reynolds number increases and the thickness of the viscous sublayer is further reduced, the presence of the superhydrophobic surface will more strongly influence the velocity profile within the viscous sublayer and reduce the momentum transferred from the fluid to the wall and the vorticity of the fluid at the edge of the viscous sublayer. Turbulence intensity is thereby reduced, increasing the drag reduction. The 60-60 ridges have better drag reduction effect compared with 30-30 ridges due to their larger microfeature spacing. Of course, saturation of the turbulent drag reduction is likely in the limit of very large Reynolds numbers where the microridges are much larger than the viscous sublayer. In this limit, the drag reduction should approach a limit of $D_R = w / (d + w)$ as momentum is only transferred from the solid fraction of the superhydrophobic surface and the viscous sublayer is thin enough that the no-slip and shear-free portions of the surface can be considered independently. For the present shear-free area ratios, this limit would be 50%.

Ruisheng Guo and Prof. Feng Zhou
Superhydrophobic Surfaces for Drag Reduction

SpringerReference
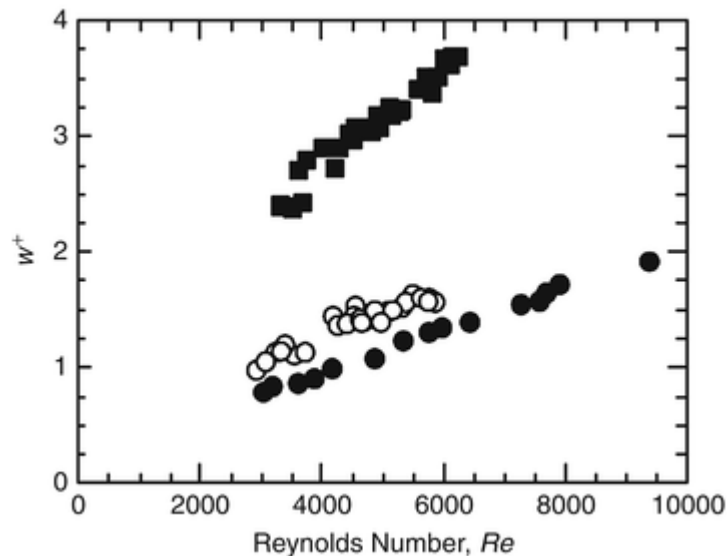
Superhydrophobic Surfaces for Drag Reduction, Fig. 7 The microridge spacing in wall units, w^+, as a function of Reynolds number. The data are taken from PIV measurements from a channel with a single superhydrophobic surface of w = 30 μm and d = 30 μm microridges (●) and from pressure measurements for flow through a channel with two superhydrophobic walls containing w = 30 μm and d = 30 μm microridges (○) and w = 60 μm and d = 60 μm microridges (·). A spacing of w^+ = 5 corresponds to the thickness of the viscous sublayer (Daniello et al. 2009)

Truesdell et al. (2006) conducted laminar Couette flow measurements near a regularly textured superhydrophobic surface and drag reduction on the order of 20% was achieved. Watanabe et al. (1999) carried out experiments on highly water-repellant walls formed by the coating of a fluoroalkane-modified acrylic resin with added hydrophobic silica. The coating resulted in a hydrophobic surface crisscrossed by microcracks of 10-20 μm in width. Pressure drop and velocity profile measurements demonstrated drag reduction up to 18% and slip lengths up to 450 μm for flows at Reynolds numbers between 500 and 10,000. Chen et al. (2010) applied superhydrophobic coating on surfaces of steel pipes, a pipe flow system was established to measure the drag and to test the durability of the micro-structure of superhydrophobic coating at average speeds varying from 1 to 6 m/s (Reynolds numbers vary from about 38,000 to 230,000). These test speeds are more practical as far as industrial applications in the real world. It is quite interesting that the superhydrophobicity of the coating shows its due characteristic of drag reduction at a higher speed for which turbulent effects are supposed to be more significant. Nevertheless, such a good feature of drag reduction at a higher speed disappeared after about 30 min.

Perspectives

In engineering applications, drag reduction by a superhydrophobic coating has been an important topic in recent years, because they can be applied in microelectromechanical systems (MEMS) and tribology devices, such as particle transport by well-technology fluids in the oil industry. The development of techniques that produce significant drag reduction in turbulent flows can have a profound effect on a variety of existing technologies. The benefits of drag reduction range from a reduction in the pressure drop in pipe flows to an increase in fuel efficiency and speed of marine vessels.

However, much room is left for further improvement and future investigations of hydrophobicity. Firstly, slippage mechanism is still under debate. Several reasons have been proposed for the slip over hydrophobic surfaces, including a molecular slip, a decrease in the viscosity of the boundary layer, the small dipole moment of a polar liquid, and a gas gap or nanobubbles at the liquid-surface interface. Here, the gas gap between the structures is used to explain the generated liquid slip. And slip length increases sharply with decreasing solid fraction and increasing effective contact angle. However, Voronov et al. (2008) demonstrated that, for hydrophobic surfaces, there is not necessarily a positive correlation between increased contact angle and slip length. So the theory of superhydrophobic drag reduction need to further study. Secondly, experimental techniques should be improved to capture the microscopic nature of slip more accurately (most importantly, a consensus of magnitude should be achieved). Because drag reduction is the ultimate goal of these studies, hydrophobic models in large size should be tested and experiments such as pressure drop in a pipe

Ruisheng Guo and Prof. Feng Zhou
Superhydrophobic Surfaces for Drag Reduction

SpringerReference

should be systematically measured. Thirdly, present experiments are mainly taken by designing two-dimensional (2D) superhydrophobic surface, while three-dimensional (3D) surface structures are rarely studied. Finally, most experiments are carried out in a low-Reynolds number channel flow at present, while the range of Reynolds number is quite large in practice. In a word, additional theories and experiments are required to achieve significant drag reduction.

Cross-References

Liquid Contact Angle Measurement
Lubrication Considering Boundary Slip
Reynolds Equation
Reynolds Number
Shear Dependence of Viscosity
Surface Free Energy
Surface Roughness

References

- W. Brostow, Drag reduction in flow: review of applications, mechanism and prediction. J. Ind. Eng. Chem. 14, 409 (2008)
- S. Chakraborty, Microfluidics and Microfabrication (Springer Science + Business Media, New York, 2010)
- J.H. Chen, C.C. Tsai, Y.Z. Kehr, L. Horng, K. Chang, L. Kuo, An experimental study of drag reduction in a pipe with superhydrophobic coating at moderate reynolds numbers. EPJ Web Conf. 6, 19005 (2010)
- C.H. Choi, C.J. Kim, Large slip of aqueous liquid flow over a nanoengineered superhydrophobic surface. Phys. Rev. Lett. 96, 066001 (2006)
- R.J. Daniello, N.E. Waterhouse, J.P. Rothstein, Drag reduction in turbulent flows over superhydrophobic surfaces. Phys. Fluids 21, 085103 (2009)
- B. Dean, B. Bhushan, Shark-skin surfaces for fluid-drag reduction in turbulent flow: a review. Philos Trans. R. Soc. A 368, 4775 (2010)
- P. Joseph, C. Cottin-Bizonne, J.M. Benoît, C. Ybert, C. Journet, P. Tabeling, L. Bocquet, Slippage of water past superhydrophobic carbon nanotube forests in microchannels. Phys. Rev. Lett. 97, 156104 (2006)
- M. Liu, L. Jiang, Switchable adhesion on liquid/solid interfaces. Adv. Funct. Mater. 20, 3753 (2010)
- X. Liu, W. Wu, X. Wang, Z. Luo, Y. Liang, F. Zhou, A replication strategy for complex micro/nanostructures with superhydrophobicity and superoleophobicity and high contrast adhesion. Soft Matter 5, 3097 (2009)
- K. Liu, X. Yao, L. Jiang, Recent developments in bio-inspired special wettability. Chem. Soc. Rev. 39, 3240 (2010)
- R. Truesdell, A. Mammoli, P. Vorobieff, F. van Swol, C. Brinker, Drag reduction on a patterned superhydrophobic surface. Phys. Rev. Lett. 97, 044504 (2006)
- O.I. Vinogradova, Drainage of a Thin Liquid Film Confined between Hydrophobic Surfaces. Langmuir 11, 2213 (1995)
- R.S. Voronov, D.V. Papavassiliou, L.L. Lee, Review of fluid slip over superhydrophobic surfaces and its dependence on the contact angle. Ind. Eng. Chem. Res. 47, 2455 (2008)
- K. Watanabe, Yanuar, H. Udagawa, Drag reduction of Newtonian fluid in a circular pipe with a highly water-repellent wall. J. Fluid Mech. 381, 225 (1999)
- W. Wu, X. Wang, D. Wang, M. Chen, F. Zhou, W. Liu, Q. Xue, Alumina nanowire forests via unconventional anodization and super-repellency plus low adhesion to diverse liquids. Chem. Commun. 1043 (2009)

Ruisheng Guo and Prof. Feng Zhou
Superhydrophobic Surfaces for Drag Reduction

SpringerReference

Superhydrophobic Surfaces for Drag Reduction

Ruisheng Guo	State Key Laboratory of Solid Lubrication, Lanzhou Institute of Chemical Physics, Chinese Academy of Sciences, Lanzhou, P. R. China
Prof. Feng Zhou	State Key Laboratory of Solid Lubrication, Lanzhou Institute of Chemical Physics, Chinese Academy of Sciences, Lanzhou, P. R. China

---